CORRELATIONS BETWEEN INTERNAL MOBILITY AND STABILITY OF GLOBULAR PROTEINS

Kurt Wüthrich, Gerhard Wagner, René Richarz, and Werner Braun, *Institut für Molekularbiologie und Biophysik, Eidgenössische Technische Hochschule, CH-8093 Zürich-Hönggerberg, Switzerland*

ABSTRACT The recent work is surveyed which leads to the suggestions that the conformation of globular proteins in solution corresponds to a dynamic ensemble of rapidly interconverting spatial structures, that clusters of hydrophobic amino acid side chains have an important role in the architecture of protein molecules, and that mechanistic aspects of protein denaturation can be correlated with internal mobility seen in the native conformation. These conclusions resulted originally from high resolution ^{1}H nuclear magnetic resonance (NMR) studies of aromatic ring mobility, exchange of interior amide protons and thermal denaturation of the basic pancreatic trypsin inhibitor and a group of related proteins. Various new approaches to further characterize proteins in solution have now been taken and preliminary data are presented. These include computer graphics to outline hydrophobic clusters in globular protein structures, high resolution ^{1}H-NMR experiments at variable hydrostatic pressure and ^{13}C-NMR relaxation measurements. At the present early stage of these new investigations it appears that the hydrophobic cluster model for globular proteins is compatible with the data obtained.

INTRODUCTION

In a series of recent papers we described high resolution proton nuclear magnetic resonance (NMR) studies of the spatial structures in solution of a group of small globular proteins related to the basic pancreatic trypsin inhibitor (BPTI) either by chemical modification (1–4) or by homology (5, 6). For all the proteins considered, the average solution conformation coincided closely with the molecular structure of BPTI seen in single crystals (7). Thus we had a quite unique system for investigating the influence of local modifications of the covalent structure on the dynamic properties and the stability of a given spatial protein structure. The strategy used in these investigations is illustrated in Fig. 1. The NMR studies concentrated mainly on measurements of amide proton exchange rates, mobility of the aromatic rings and protein denaturation (8–13). Presently these earlier data are being complemented by various different experiments to investigate additional aspects of protein conformation in solution. This includes high resolution ^{1}H-NMR experiments at high hydrostatic pressure, computer graphics for detailed inspection of protein structures and measurements of nuclear spin relaxation times. Preliminary data obtained from these different approaches are discussed in the light of the previously suggested multi-state cluster description of globular proteins (9–11).

METHODS

^{1}H-NMR spectra at 360 MHz and ^{13}C-NMR spectra at 90.5 MHz were recorded on a Bruker HX 360 spectrometer. ^{13}C-NMR spectra at 25.1 MHz were obtained with a Varian XL-100 spectrometer. Experimental details on the sample preparation and the NMR techniques used were presented previously (1–6, 12, 13). High resolution 360 ^{1}H-NMR spectra at variable hydrostatic pressure were obtained with a home-built experimental device using a thick-walled glass capillary as a sample cell. A

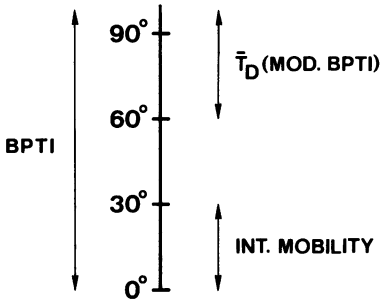

Figure 1 Strategy for the investigations of BPTI-related proteins. In aqueous solution the globular conformation of BPTI is stable over the temperature range from 0° to >95°C. Different, strictly localized modifications of the covalent structure yielded proteins with average denaturation temperature $\bar{T}_D$ between 60° and 95°. It was then investigated whether the variations of T_D could be correlated with the internal flexibility of the globular protein structures manifested e.g. in the exchange of interior labile protons and in intramolecular rotational motions of the aromatic rings at temperatures far below $\bar{T}_D$.

detailed description of the high pressure apparatus, which was based on principles outlined by Yamada (14) and Volkl et al. (15), will be given elsewhere.[1]

For the computer graphics studies we made use of the "Zentrum für Interaktives Rechnen" of the ETH. A DEC-10 computer was used with the program XRAY[2] to produce molecular models from a protein structure data bank. A PDP-11 computer with Evans and Sutherland picture system PS 2 was used with the program PROT[2] to orient the protein molecules to get the most informative views.

RESULTS

Amide Proton Exchange, Aromatic Ring Mobility, and Thermal Stability of Native and Chemically Modified BPTI

The structures of BPTI and a group of related proteins obtained by strictly localized chemical modifications are described in Fig. 2. Data on internal mobility and stability of these proteins are presented in Table I. Since the spin systems of all the eight aromatic rings (1–6) and the resonances of numerous amide protons (16, 17) were individually assigned, the data on internal rate processes could be correlated with specific locations in the protein structure. The following are some key observations made in these experiments.

The exchange rates of interior labile protons are correlated with the thermal stability of the proteins, i.e., at a given temperature the exchange rates were higher in the less stable proteins (Table I). In contrast, the mobility of the aromatic rings was not noticeably affected by localized chemical modifications (Fig. 2), unless the modification involved the immediate ring environment.

Different amide protons in the BPTI-related proteins exchanged with different rates (12). Overall, the protons of the β-sheet exchanged more slowly than those of the α-helix. Within the β-sheet the exchange was faster at both ends than in the central region. Similarly, different rates of the flipping motions about the C^{β}-C^{γ} bond were observed for the individual aromatic rings (18).

As a consequence of the chemical modifications in Fig. 2, the amide proton exchange rates were increased by several orders of magnitude (Table I). In contrast to these large differences

[1]G. Wagner, manuscript submitted for publication.

[2]The programs XRAY and PROT were adapted from programs which were kindly provided to us by Richard M. Feldmann, National Insitutes of Health, Bethesda, Md. 20205.

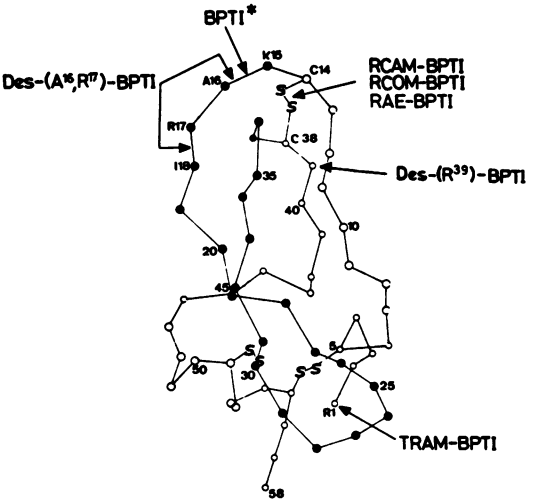

Figure 2 Projection of the α-carbon positions in the BPTI molecule obtained from a single crystal x-ray analysis (7). The structure contains three disulfide bonds, a twisted antiparallel β-sheet which extends through the entire length of the molecule, and a short α-helix near the C-terminus. The disulfide bonds are included in the drawing and the residues in the antiparallel β-sheet are identified by filled circles. The arrows indicate the locations of the chemical modifications discussed in this paper. Amino acid residues in the modification sites are identified by the IUPAC one-letter symbol and the position in the amino acid sequence. RCAM-BPTI, RCOM-BPTI and RAE-BPTI were obtained by reduction of the disulfide bond 14–38, with the cysteinyl residues protected by carboxamidomethylation, carboxymethylation or aminoethylation, respectively: BPTI* was obtained by cleavage of the peptide bond Lys 15—Ala 16, Des (A^{16}, R^{17})-BPTI by cleavage of the peptide bond Lys 15—Ala 16 and removal of Ala 16 and Arg 17, TRAM-BPTI by transamination of the α-amino group of Arg 1, and Des-(R^{39})-BPTI by cleavage of the peptide bond Arg 39—Ala 40 and removal of Arg 39. BPTI contains eight aromatic residues, i.e. four phenylalanines in the positions 4, 22, 33, and 45, and four tyrosines in the positions 10, 21, 23, and 35.

between the absolute rates, the rank order of the exchange of individual protons was with few exceptions identical in the different proteins. Thus, even though most of the chemical modifications were in peripheral locations in the molecular structure, e.g., at the *N*-terminus or at the reactive-site peptide bond, they caused an increase of the exchange rates throughout the entire protein. For each individual one of the interior amide protons, the exchange followed EX_2 kinetics (19) over the entire p^2H range studied (12).

TABLE I
THERMAL STABILITY AND INTERNAL MOBILITY OF BPTI-RELATED PROTEINS IN AQUEOUS SOLUTION

Protein	$\overline{T_D}$ [°C] [p^2H 5.0]	k^{NH} [min^{-1}] [p^2H 4.5, 36°C]	Phe-45 [p^2H 7.8, 4°C]	
			ν[s^{-1}]	$\Delta G^{\ddagger}$ [kJ mol^{-1}]
BPTI	>95	2×10^{-7}	30	60
TRAM-BPTI	[~95]	[$>2 \times 10^{-7}$]	30	60
BPTI*	85	5×10^{-5}	60	58
Des-(R^{39})-BPTI	85	3×10^{-4}	30	60
RCOM-BPTI	79	4×10^{-4}	30	60
RCAM-BPTI	76	1×10^{-4}	30	60
RAE-BPTI	70	6×10^{-4}	30	60
DES-(A^{16},R^{17})-BPTI	>65	7×10^{-5}	60	58

The table lists the average denaturation temperature $\overline{T_D}$, the exchange rate constant, k_{ex}^{NH}, for the most slowly exchanging amide proton, and the frequency ν and activation energy $\Delta G^{\ddagger}$ of the 180° flips of the Phe 45 ring about the C^{β}-C^{γ} bond.

When different separated resonance lines were observed through the thermal denaturation, differences of the order of up to 4° were found between the apparent denaturation temperatures for individual protons (20).

Since these resonances were previously individually assigned (21) the different denaturation behavior could be correlated with specific regions of the molecule. A general trend was that the α-protons of the polypeptide backbone showed lower apparent denaturation temperatures than the protons of hydrophobic side chains.[3]

High Resolution ^{1}H-NMR at High Hydrostatic Pressure

Since reaction volumes, ΔV, in chemical equilibria with equilibrium constant K are given by

$$\Delta V = -RT\frac{d\ ln\ K}{dp}$$

and activation volumes, $\Delta V^{\ddagger}$, in rate processes with rate constant k by

$$\Delta V^{\ddagger} = -RT\frac{d\ ln\ k}{dp},$$

investigations at variable hydrostatic pressure, p, can provide essential data for the characterization of thermodynamic and mechanistic aspects of protein conformation in solution. We have started measurements of the dependence of the parameters of Table I on hydrostatic pressure in the range from 1 to 2,500 atm.

At present quantitative data were obtained for the rotational motions of the aromatic rings of Tyr 35 and Phe 45 in BPTI. The activation volumes, $\Delta V^{\ddagger}$, for 180° flips of these two rings about the C^{β} - C^{γ} bond (8, 22) were found to be 63 ± 20 Å^3 and 50 ± 10 Å,^{3} respectively.[1] Positive activation volumes for rotational motions of interior aromatic rings in globular proteins appear not to be unique for BPTI, since similar results were obtained for three aromatic rings in ferricytochrome *c*.[1]

^{13}C-NMR Relaxation Studies

To complement the results on the internal mobility of BPTI-related proteins in Table I by measurements on a different time scale, the ^{13}C-relaxation times T_1 and T_2 and the ^{13}C [^{1}H]NOE (8) were studied at 25.1 MHz and 90.5 MHz (23).[4]

The main emphasis was on studies of backbone α-carbons, aromatic ring carbons, and methyl carbons of aliphatic amino acid side chains, which had previously been individually assigned (23, 24). An analysis of these data in terms of a "wobbling-in cone" model (23, 25)[4] indicated that, in addition to the rapid methyl rotation, the methyl carbon relaxation times manifest librational motions of the side chains with correlation times of the order of 10^{-9} s and with angular displacements of 20°–50°.

Here we present an empirical comparison of relaxation data for BPTI and RCAM-BPTI. Table II shows that within the accuracy of these experiments no significant differences between the T_1 values of corresponding carbons in the two proteins were observed. Hence

---

[3]The same trend was since observed in several snake neurotoxins and cardiotoxins. In certain toxins the differences between the apparent denaturation temperatures for backbone α-protons and aromatic ring protons is considerably larger than 5°C. A. Chrzeszczyk, Ch. Moonen, J. Lauterwein, M. Lasdunski, W. Steinmetz, L. Visser, G. Wider, and K. Wüthrich, unpublished data.

[4]Richarz, R., K. Nagayama, K. and K. Wüthrich. Manuscript submitted for publication.

TABLE II

RELAXATION TIMES T_1 (msec) OF SELECTED ^{13}C-RESONANCE LINES IN BPTI AND RCAM-BPTI AT 25.1 MHz, p^2H = 4.1, T = 39°C.

Resonance Assignments	T_1	
	BPTI	RCAM-BPTI
α-carbons (average)	45 ± 3	48 ± 3
Tyr ε (average)	46 ± 3	45 ± 5
Ala 16 β	160 ± 20	180 ± 30
Ala 40 β		—
Ala 27 β	150 ± 20	160 ± 20
Ala 48 β	150 ± 20	160 ± 20
Ala 58 β	~300	300 ± 30
Ile 18 γ^2	215 ± 30	170 ± 20
Ile 19 γ^2	215 ± 30	200 ± 20
Ile 18 δ	385 ± 30	360 ± 40
Ile 19 δ	290 ± 30	240 ± 30
Met 52 ε	325 ± 30	330 ± 30

The relaxation times were measured with the inversion recovery method (26) in $2.5 \cdot 10^{-2}$ M solutions of the protein in ^2H_2O.

there was no apparent correlation between internal segmental motions on the nanosecond time scale and the thermal stability of the globular proteins (Table I).

DISCUSSION

Multi-State Hydrophobic Cluster Model for Globular Proteins

Fig. 3 shows a scheme of fundamental structural aspects of a dynamic multistate model for globular proteins which was suggested on the basis of the data in Table I and additional observations (9–11, 27). The fundamental point in Fig. 3 is that the protein molecule consists of hydrophobic clusters which are loosely connected by covalent bonds and held in fixed

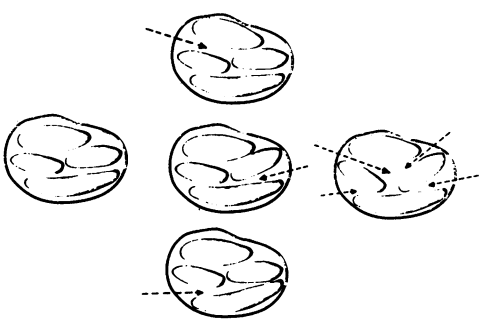

Figure 3 Schematic two-dimensional representation of a dynamic multistate model for globular proteins. Clusters formed by hydrophobic side chains are the pillars of the molecular structure. The individual clusters are loosely linked together by the polypeptide backbone and interact primarily via polar groups located on their surfaces, e.g., by hydrogen bonding. In the compact average structure on the left, interior amide protons in the interfaces between different clusters are shielded from the solvent. The three species in the center represent distorted structures contained in the molecular conformation at temperatures far below the denaturation point. Through variations of the relative spatial orientations of the intact clusters, individual interior amide protons are exposed to the solvent, as indicated by the arrows. The drawing on the right represents a more strongly distorted open structure which would be characteristic for the species prevailing near denaturing conditions.

spatial orientations mainly by interactions between polar groups on the cluster surfaces, i.e., primarily hydrogen bonded secondary structures. Transitions between the molecular structures contained in the protein conformation are by two different types of intramolecular fluctuations which promote, respectively, exchange of interior amide protons or rotational motions of the aromatic rings: (*a*) Translational and rotational motions of the intact hydrophobic clusters relative to each other primarily expose labile protons on the interior surface of the clusters to the solvent, thus enabling exchange to take place. These are "global" fluctuations of the protein structure in the sense that they are related to the thermal stability and that a localized variation of the covalent structure affects nearly identically the exchange rates of all amide protons throughout the protein (13). (*b*) Structure fluctuations within the hydrophobic clusters determine the mobility of the aromatic rings, since these are located in the interior of the clusters. The experiments showed that the fluctuations manifested in the ring flips were strictly localized, i.e. not correlated with the stability of the protein and not susceptible to long range effects from chemical modifications (9–11). The observations of different apparent denaturation temperatures for backbone fragments on the surface of the clusters and for different hydrophobic amino acid side chains located in different clusters could be explained with the assumption that cooperative unfolding in the structure of Fig. 3 extends only over the individual clusters. In a first phase of the process of unfolding the regions of contact between the different clusters would be altered, which would be followed by cooperative decay of individual clusters (20). The new experiments described in this paper were designed to provide additional criteria for distinguishing between different types of internal fluctuations of protein structures and for characterization of the hydrophobic clusters in Fig. 3.

Measurements of the activitation volumes, $\Delta V^{\ddagger}$, for the aromatic ring flips and the amide proton exchange appear to provide additional evidence that these two rate processes are correlated with different types of internal fluctuations of the protein structure. While we measured positive $\Delta V^{\ddagger}$'s for the ring flips, Carter et al. (28) reported small positive and negative $\Delta V^{\ddagger}$ for proton exchange in aqueous solutions of different proteins. ^{1}H-NMR measurements of $\Delta V^{\ddagger}$ for the exchange of individual amide protons in BPTI, where the same pressure range will be covered as for the studies of the ring flips,[1] are in progress in our laboratory. A reliable check of the above conclusion should thus soon be available.

Measurements of $\Delta V^{\ddagger}$ are also a potential source of information on the mechanism of the aromatic ring flips (22, 29). Positive values for $\Delta V^{\ddagger}$ show that the ring flips occur when the protein adopts a larger than average volume. It is then interesting that the $\Delta V^{\ddagger}$'s measured for Tyr 35 and Phe 45 correspond approximately to the volume of the atoms near the rings which stick into the sphere occupied by the rotating ring (22). This may indicate that the "viscosity" of the ring environment, as defined in (29), does not have a dominant influence during the actual process of ring rotation.

For the analysis of the ^{13}C-relaxation data in Table II it is essential that previous studies showed the average solution structures of BPTI and RCAM-BPTI to be closely similar. Hence the correlation times for overall rotational motions should be nearly identical and different relaxation times would thus manifest different librational mobility for corresponding groups in the two proteins. Similar to the aromatic ring flips (Table I) the librational motions of the backbone and the aliphatic amino acid side chains thus appear to manifest internal fluctuations of the protein structure which are not correlated with the thermal stability of the globular structure. Interestingly most of the methyl carbon resonances in Table II correspond to amino acid side chains located near the aromatic rings in the hydrophobic clusters.

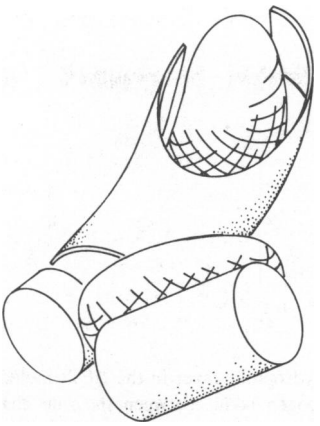

Figure 4 Schematic presentation of the hydrophobic cluster structure of BPTI. Two hydrophobic clusters, which are characterized in more detail in Fig. 5, a hydrophilic layer, which is described in detail in Fig. 6, and two helices are distinguished. A hydrophobic cluster which contains the side chains of Phe 23, Phe 33, and Tyr 35 is surrounded by the hydrophilic layer. The second cluster between the hydrophilic layer and the C-terminal helix includes the side chains of Phe 4, Tyr 21, Tyr 23, and Phe 45. The short *N*-terminal helix has direct H-bond connections to the hydrophilic layer.

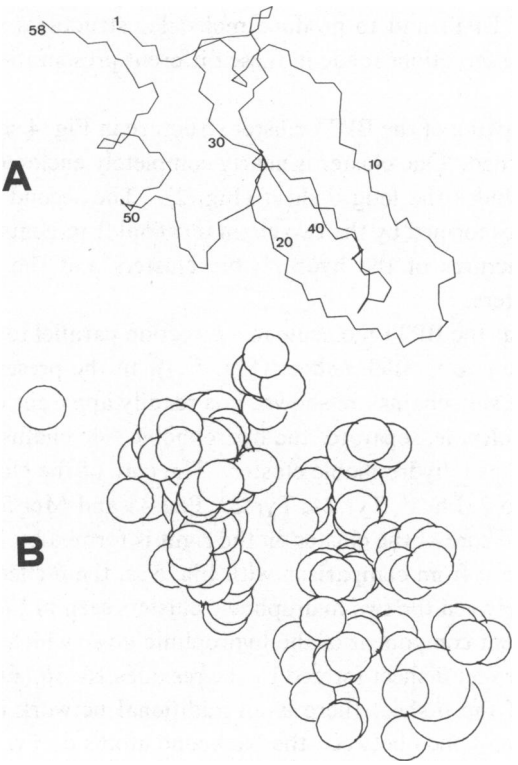

Figure 5 Computer drawing of hydrophobic clusters in BPTI. The orientation of the molecule resulted from rotations by 40°, 22°, and 100°, respectively, about the fixed x-, y-, and z-axes used by Deisenhofer and Steigeman (7). Trace *A* shows a line drawing of the polypeptide backbone from this point of view. *B* presents a space filling drawing of the side chains of Ala, Val, Leu, Ile, Pro, Met, Cys, Phe, and Tyr. No backbone atoms are shown except for the α-carbons and the amide nitrogens of Pro. Atomic radii of 1.5, 1.65, and 2.5 Å were used for C, N, and S, hydrogen and oxygen atoms are not shown.

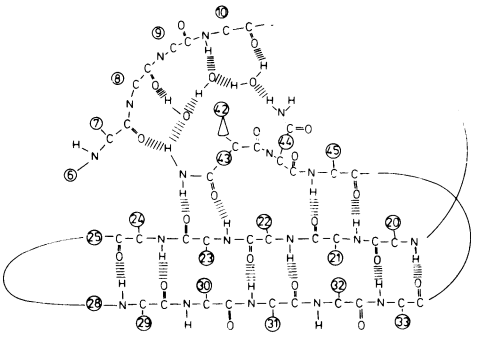

Figure 6 Planar projection of the hydrophilic layer in the BPTI molecule (Fig. 4). This layer includes the triple-stranded β-sheet and hydrogen bonds between the side chains of Asn 43 and Asn 44, the backbone fragment 7–10 and three internal water molecules (7). The α-carbons are identified by the position of the residues in the amino acid sequence (5–7). The α-protons are not shown. Residues 8 and 9 are prolines. Only the central region of the β-sheet is shown (see Fig. 2). The peptide bond 41–42 points out of the plane of projection. The missing protons of the water molecules are located above the projection plane.

Hydrophobic Clusters in the Crystal Structure of BPTI

The atomic coordinates of Deisenhofer and Steigemann (7) were used to construct a "Labquip" model of BPTI and to produce molecular structures with a computer graphics system. The major observations made in these different presentations of BPTI are illustrated in Figs. 4–6.

The schematic drawing of the BPTI cluster structure in Fig. 4 shows that two hydrophobic clusters can be discerned. One cluster is nearly completely enclosed by a layer of hydrophilic fragments which includes the long β-sheet (Fig. 2). The second cluster is enclosed by the β-sheet and the helices formed by the two chain terminal fragments. Figs. 5 and 6 describe in more detail the structures of the hydrophobic clusters and the hydrophilic layer located between the two clusters.

In Fig. 5 we look at the BPTI molecule in a direction parallel to the hydrogen bonds of the central portion of the antiparallel β-sheet (Fig. 5 *A*). In the presentation of Fig. 5 *B*, where only the hydrophobic side chains are shown, it is readily apparent that a cleft, which extends through the entire molecule, separates the hydrophobic side chains into two groups. Each of the two groups contains a hydrophobic cluster. The core of the cluster on the left consists of the side chains of Pro 2, Phe 4, Tyr 21, Tyr 23, Phe 45 and Met 52, and the disulfide bonds 5–55 and 30–51. The core of the cluster on the right is formed by Pro 9, Phe 22, Phe 33, and Tyr 35. As can be seen from comparison with Fig. 5 *A*, the β-sheet of the BPTI structure is located in the cleft between the two hydrophobic clusters seen in Fig. 5 *B*.

The most prominent component of the hydrophilic layer which separates the two clusters (Fig. 4) is the antiparallel β-sheet formed by the residues 16–36 (Fig. 2). Fig. 6 shows that in the central region of the β-sheet there is an additional network of hydrogen bonded polar groups. The hydrogen bonds between the backbone atoms of Tyr 21 and Phe 45 produce a short stretch of triple stranded β-sheet, and the side chain of Asn 43 is hydrogen bonded to the backbone atoms of Tyr 23 in the β-sheet. The side chains of Asn 43 and Asn 44 are then, via three interior water molecules, connected to the backbone fragment 7–10 and to the short *N*-terminal helix (Fig. 4). This hydrophilic layer essentially divides the molecule into two parts. In its shape it resembles a half barrel which encloses one of the hydrophobic clusters (Fig. 4).

Overall, inspection of the crystal structure of BPTI thus revealed features which appear to be compatible with the hydrophobic cluster architecture suggested by the solution studies (Fig. 3). Fig. 4 would in particular provide an explanation for the thermal denaturation studies, which so far has allowed us to distinguish three different apparent denaturation temperatures for individual polypeptide fragments (20). On the basis of the individual resonance assignments the three different denaturation temperatures could be correlated with the two clusters and the contact area between the clusters.

Use of the facilities at the Zentrum für Interaktives Rechnen (ZIR) of the ETH is gratefully acknowledged. Financial support was obtained from the Schweizerischer Nationalfonds (project. 3.0046.76). W. Braun was the recipient of a fellowship from the Schweizerische Kommission für Molekularbiologie (SKMB). We would like to thank H. Roder and M. Meier for the preparation of the large quantities of RCAM-BPTI needed for the ^{13}C-NMR experiments.

Received for publication 29 November 1979.

REFERENCES

1. Brown, L. R., A. De Marco, R. Richarz, G. Wagner, and K. Wüthrich. 1978. The influence of a single salt bridge on static and dynamic features of the globular solution conformation of the basic pancreatic trypsin inhibitor. ^{1}H and ^{13}C nuclear-magnetic-resonance studies of the native and the transaminated inhibitor. *Eur. J. Biochem. 88:87–95.*
2. Wagner, G., H. Tschesche, and K. Wüthrich. 1979. The influence of localized chemical modifications of the basic pancreatic trypsin inhibitor on static and dynamic aspects of the molecular conformation in solution. *Eur. J. Biochem.* **95**:239–248.
3. Wagner, G., A. J. Kalb(Gilboa) , and K. Wüthrich. 1979. Conformational studies by ^{1}H nuclear magnetic resonance of the basic pancreatic trypsin inhibitor after reduction of the disulfide bond between Cys-14 and Cys-38. *Eur. J. Biochem.* **95**:249–253.
4. Richarz, R., H. Tschesche, and K. Wüthrich. 1980. Structural characterisation by nuclear magnetic resonance of a reactive site-carbon-13 labelled basic pancreatic trypsin inhibitor with the peptide bond Arg-39-Ala-40 cleaved and Arg-39 removed. *Eur. J. Biochem.*. In press.
5. Wagner, G., K. Wüthrich, and H. Tschesche. 1978. A ^{1}H nuclear-magnetic-resonance study of the conformation and the molecular dynamics of the glycoprotein cow-colostrum trypsin inhibitor. *Eur. J. Biochem.* **86**:67–76.
6. Wagner, G., K. Wüthrich, and H. Tschesche. 1978. A ^{1}H nuclear-magnetic resonance study of the solution conformation of the isoinhibitor K. from Helix pomatia. *Eur. J. Biochem.* **89**:367–377.
7. Deisenhofer, J., and W. Steigemann. 1974. Crystallographic refinement of the structure of bovine pancreatic trypsin inhibitor at 1.5 resolution. *Acta Crystallographica B.* **31**:238–250.
8. Wüthrich, K. 1976. NMR in Biological Research: Peptides and Proteins. Elsevier-North Holland Publishing Co., Amsterdam. 1–379.
9. Wagner, G., and K. Wüthrich. 1978. Dynamic model of globular protein conformations based on NMR studies in solution. *Nature (Lond.).* **275**:247–248.
10. Wüthrich, K. and G. Wagner. 1978. Internal motions in globular proteins. *Trends Biol. Sci.* **3**:227–230.
11. Wüthrich, K., G. Wagner, and R. Richarz. 1978. A dynamic model for globular protein conformations based on high resolution NMR data. *In* Protein: Structure, Function and Industrial Applications, Proceedings of the 12th FEBS Meeting, Dresden 1978. E. Hofmann, W. Pfeil and H. Aurich, editors. **52**:143–152.
12. Richarz, R., P. Sehr, G. Wagner, and K. Wüthrich. 1979. Kinetics of the exchange of individual amide protons in the basic pancreatic trypsin inhibitor. *J. Mol. Biol.* **130**:19–30.
13. Wagner, G., and K. Wüthrich. 1979. Correlation between the amide proton exchange rates and the denaturation temperatures in globular proteins related to the basic pancreatic trypsin inhibitor. *J. Mol. Biol.* **130**:31–37.
14. Yamada, H. 1974. Pressure resisting glass cell for high pressure, high resolution NMR measurements. *Rev. Sci. Instrumen.* **45**:640–642.
15. Völkl, G., E. Lang, and H. D. Lüdemann. 1979. High-resolution nuclear magnetic resonance III: Concentration dependence of $\Delta V^{\ddagger}$ and $\Delta G^{\ddagger}$ for the rotation of the dimethylaminogroup in aqueous solutions of some N,N-dimethylamides. *Ber. Bunsenges. Phys. Chem.* **83**:722–729.
16. Marinetti, T. D., G. H. Snyder, and B. D. Sykes. 1976. Nuclear magnetic resonance determination of intramolecular distances in bovine pancreatic trypsin inhibitor using nitrotyrosine chelation of lanthanides. *Biochemistry* **15**:4600–4608.

17. Dubs, A., G. Wagner, and K. Wüthrich. 1979. Individual assignments of amide proton resonances in the proton NMR spectrum of the basic pancreatic trypsin inhibitor. *Biochim. Biophys. Acta.* **177–194.**
18. Wagner, G., A. De Marco, and K. Wüthrich. 1976. Dynamics of the aromatic amino acid residues in the globular conformation of the basic pancreatic trypsin inhibitor (BPTI). I. ^{1}H-NMR studies. *Biophys. Struct. Mech.* **2**:139–158.
19. Hvidt, A., and S. O. Nielsen. 1966. Hydrogen exchange in proteins. *Adv. Protein Chem.* **21**:287–386.
20. Wüthrich, K., H. Roder, and G. Wagner. 1979. Internal mobility and unfolding of globular proteins. *In* Protein Folding. R. Jaennicke, editor. Elsevier-North Holland Biomedical Press, Amsterdam. In press.
21. Wüthrich, K., and G. Wagner. 1979. Nuclear magnetic resonance of labile protons in the basic pancreatic trypsin inhibitor. *J. Mol. Biol.* **130**:1–18.
22. Hetzel, R., K. Wüthrich, J. Deisenhofer, and R. Huber. 1976. Dynamics of the basic pancreatic trypsin inhibitor (BPTI). II. Semi-empirical energy calculations. *Biophys. Struct. Mech.* **2**:159–180.
23. Richarz, R. 1979. ^{13}C Kernresonanzstudien an kleinen Modellpeptiden sowie am Basischen Pankreatischen Trypsin Inhibitor und seinem Komplex mit Proteasen. Ph.D. Thesis, ETH Zurich. No. 6495.
24. Richarz, R., and K. Wüthrich. 1978. High-field ^{13}C nuclear magnetic resonance studies at 90.5 MHz of the basic pancreatic trypsin inhibitor. *Biochemistry* **17**:2263–2269.
25. Kinosita, K., Jr., S. Kawato, and A. Ikegami. 1977. A theory of fluorescence polarisation decay in membranes. *Biophys. J.* **20**:289–305
26. Freeman, R., and H. D. W. Hill. 1969. High-resolution studies of nuclear spin-lattice relaxation. *J. Chem. Phys.* **51**:3140.
27. Wagner, G., and K. Wüthrich. 1979. Structural interpretation of the amide proton exchange in the basic pancreatic trypsin inhibitor and related proteins. *J. Mol. Biol.* **134**:75–94.
28. Carter, J. V., D. G. Knox, and A. Rosenberg. 1978. Pressure effects on folded proteins in solution. *J. Biol. Chem.* **253**:1947–1953.
29. McCammon, J. A., P. G. Wolynes, and M. Karplus. 1979. Picosecond dynamics of tryrosine side chains in proteins. *Biochemistry* **18**:927–942.

DISCUSSION

Session Chairman: Hans Frauenfelder *Scribe*: Carolyn Ritz-Gold

FRAUENFELDER: We have an extended comment from Joseph Rosa.

ROSA: We have observed the exchange behavior of the S-protein of RNAse S. The results extend some of the findings described here for BPTI. We looked at exchange rates as a function of pH, temperature and S-peptide binding using a tritium exchange method that yields average rates for known local regions of the protein. The details of the method have been published by Rosa and Richards (1979, *J. Mol. Biol.*, **133**:399–416). The portions of S-protein whose exchange rates we monitored included regions of α-helix, β-sheet and the C-terminal tetrapeptide.

From the rate of exchange of the isolated S-protein, we found that at pH 2.8 all these fragments had at least one site exchanging relatively slowly. Based on the increase in (OH^-), the exchange rates in going from pH 2.8 to pH 5.35 would be predicted to be ~100 times greater than the rates at pH 2.8. Depending on the fragment, the rates of exchange at pH 5.35 were, however, observed to be only 2–4 times greater. Similarly, the rates of exchange at pH 7 would be predicted to be 35–45 times greater than rates at pH 5.35, but the observed rates at pH 7 were only 5–20 times greater.

This apparent violation of first-order dependence on pH is undoubtedly due to the dramatic increase in the thermal stability of the S-protein at pH 7 compared to pH 2.8. These results therefore point to a similar correlation of exchange rates with thermal stability as that observed for BPTI. The relative exchange rates are presumably linked to the relative thermal stability by intramolecular "vibrational" modes. They are probably not normal modes in the usual sense and may or may not be present in the type of picosecond simulation presented here by McCammon and Karplus.

This pH dependence and correlation with thermal stability also correlates well with Jim Matthew's electrostatic calculations. This kind of argument linking exchange rates to thermal stability via either a distribution of microstates or oscillatory modes is also consistent with the temperature dependence of the exchange rates. If activation energy is plotted vs. temperature, we see from the activation energy at pH 2.8, e.g., that even at low temperature, many degrees of freedom would be populated at the level of kT. We would also predict that exchange would be mediated by a low energy process.

If the thermal stability of the protein is increased, e.g. by going to pH 5.35, we would predict that the electrostatic interactions presumably contributing to the thermal stability and tightening the protein will have local interactions and effectively increase the force constants of the "springs" contributing to these degrees of freedom. We would